GSA Data Repository DR2009128

Day *et al.* (2009) Pyroxenite-rich mantle formed by recycled oceanic lithosphere: oxygen-osmium isotope evidence from Canary Island lavas

Supplementary Methods

Oxygen isotope analyses were performed on visibly fresh, inclusion-free olivine. Olivines were separated from their rock matrix by crushing and sieving, followed by hand separation with the aid of a binocular microscope. The resultant separates were rigorously cleaned to remove adhering matrix materials using an ultrasonic bath and ultra-pure MQ-H_2O and methanol reagents. $\delta^{18}O$ values ($\delta^{18}O_n$ is the per mil [‰] deviation of $^{18}O/^{16}O$ in *n* from the international standard [std] V-SMOW given by the relationship: $\delta^{18}O_n = 1000 \times (^{18}O/^{16}O_n / ^{18}O/^{16}O_{std} - 1)$) were measured at Royal Holloway, University of London on 1 to 2 mg splits using the laser fluorination protocols of Mattey (1997). Yields for all unknowns and standards in this study were 98 ± 2%. Precision and accuracy of analyses was monitored with three internal standards; two different olivines from San Carlos and the UW GMG 2 garnet standard. The isotopic composition of these minerals relative to the international standard biotite NBS-30, and deviations of replicate analyses over the analytical period were: RHUL SCOL I +4.84‰ (± 0.16, 2σ, *n* = 27), RHUL SCOL II +5.22‰ (± 0.16, 2σ, *n* = 19) and UW GMG 2 garnet +5.71‰ (± 0.18, 2σ, *n* = 22). These values are in excellent agreement with previously published values for these standard materials (Sharp, 1990; Valley *et al.,* 1995; Eiler *et al.,* 2000; Wang and Eiler, 2008).

Osmium isotope and Re and Os abundance analyses were performed on 1 to 2g of whole-rock powder using procedures described in Pearson and Woodland (2000) and Day *et al.* (2008). Briefly, this included digestion in Carius tubes, with an enriched Re-Os spike and ≥9 mL of inverse Aqua Regia at ~240ºC for >72 hours. Os was triply extracted from the inverse Aqua Regia using CCl_4 and then back-extracted into HBr, prior to purification via micro-distillation. Re was recovered and purified from the residual solutions using an anion-exchange column separation technique. Os isotopic compositions were measured via N-TIMS on a Triton mass spectrometer. Re was measured using an ELAN 6000 Quadrupole ICP-MS and a Neptune MC-ICP-MS. All Os isotope values are oxide, fractionation, spike and blank corrected. External precision for $^{187}Os/^{188}Os$ over the course of the study was better than 2.1‰ (2σ) on the Durham Triton for two separate standards of variable load sizes provided by the University of Maryland (UMCP standard) and Carnegie Institution of Washington (DTM standard); 0.017-3.5ng load sizes; UMCP = 0.11382 ± 0.00024, 2σ, *n* = 273; DTM = 0.17402 ± 0.00027, 2σ, *n* = 21. Precision and reproducibility of this technique, including presentation of analysed reference material GP13 run during the course of this study, is outlined in Day *et al.* (2008). Total procedural blanks (*n* = 10) had an average $^{187}Os/^{188}Os$ isotope composition of 0.22 ±0.05, with average concentrations of 2.9 ±1.9pg [Re] and 0.5 ±0.2pg [Os] (1σ). All samples are blank corrected, with blank contributions being generally negligible.

Data Repository Figure Captions

Figure DR1 – Relative compatibility of osmium and rhenium. Whole-rock MgO (wt.%) versus (a) Os and (b) Re abundances (in ppb) for La Palma and El Hierro lavas. The positive correlation of Os with MgO is consistent with Os being situated in early-formed mineral phases trapped within olivine. Negative correlation between MgO and Re is consistent with Re acting as a moderately incompatible element during fractional crystallization.

Figure DR2 – Assessing assimilation and fractional-crystallization processes in Canary Island lavas. Whole-rock MgO (wt. %) versus (a) $^{187}Os/^{188}Os$ and (b) $\delta^{18}O_{olivine}$ for La Palma and El Hierro lavas. Lack of correlation between $^{187}Os/^{188}Os$ and $\delta^{18}O_{olivine}$ versus MgO lend support to O-Os isotope systematics of western Canary Islands reflecting mantle source variations, and not assimilation/fractional-crystallization processes.

Data Repository References Cited

Dale, C.W., Gannoun, A., Burton, K.W., Argles, T.W., and Parkinson, A.J., 2007, Rhenium-osmium isotope and elemental behaviour during subduction of oceanic crust and implications for mantle recycling: Earth and Planetary Science Letters, v. 253, p. 211-225.

Day, J.M.D., 2004, A helium, oxygen and rhenium-osmium isotope study of some intraplate magmatism [Ph.D. Thesis]. Durham, UK, University of Durham, 430p.

Day, J.M.D., Pearson, D.G., and Hulbert, L.J., 2008, Rhenium-osmium isotope and platinum-group element constraints on the origin and evolution of the 1.27 Ga Muskox Intrusion: Journal of Petrology, v. 49, p. 1255–1295.

Eiler, J.M., 2001, Oxygen isotope variations of basaltic lavas and upper mantle rocks: Reviews in Mineralogy and Geochemistry, v. 43, p. 319-364.

Eiler, J.M., Crawford, A., Elliott, T., Farley, K.A., Valley, J.W., and Stolper, E.M., 2000, Oxygen isotope geochemistry of oceanic-arc lavas: Journal of Petrology, v. 41, p. 229-256.

Lassiter, J.C., and Hauri, E.H., 1998, Osmium-isotope variations in Hawaiian lavas: evidence for recycled oceanic lithosphere in the Hawaiian plume: Earth and Planetary Science Letters, v. 164, p. 483-496.

Mattey, D.P., 1997, Micromass Application Note, v. 107, 8pp.

Nikogosian, I., Elliott, T., and Touret, J.L.R., 2002, Melt evolution beneath thick lithosphere a magmatic inclusion study of La Palma, Canary Islands: Chemical Geology, v. 183, p. 169-193.

Pearson, D.G., and Woodland, S.J., 2000, Solvent extraction/ anion exchange separation and determination of PGEs (Os, Ir, Pt, Pd, Ru) and Re-Os isotopes in geological samples by isotope dilution ICP-MS: Chemical Geology, v. 165, p. 87–107.

Pearson, D.G., and Nowell, G.M., 2004, Re-Os and Lu-Hf isotopic constraints on the origin and age of pyroxenites from the Beni Bousera peridotite massif: implications for mixed peridotite-pyroxenite mantle sources: Journal of Petrology, v. 45, p. 439-455.

Pearson, D.G., Davies, G.R., Nixon, P.H., Greenwood, P.B., and Mattey, D.P., 1991, Oxygen isotope evidence for the origin of pyroxenites in the Beni Bousera peridotite massif, N. Morrocco: derivation from subducted oceanic lithosphere: Earth and Planetary Science Letters, v. 102, p. 289-301.

Schaefer, B.F., Turner, S., Parkinson, I., Rogers, N., and Hawkesworth, C.J., 2002, Evidence for recycled Archaean oceanic mantle lithosphere in the Azores plume: Nature, v. 420, p. 304-307.

Sharp, Z.D., 1990, A laser based microanalytical method for the in situ determination of oxygen isotope ratios of silicates and oxides: Geochimica et Cosmochimica Acta, v. 54, p. 1353-1357.

Turner, S., Tonarini, S., Bindeman, I., Leeman, W.P., and Schaefer, B.F., 2007, Boron and oxygen isotope evidence for recycling of subducted components over the past 2.5 Gyr: Nature, v. 447, p. 702-705.

Valley, J.W., Kitchen, N., Kohn, M.J., Ninedorf, C.R., and Spicuzza, M.J., 1995, UWG-2, a garnet standard for oxygen isotope ratios: strategies for high precision and accuracy with laser heating: Geochimica et Cosmochimica Acta, v. 59, p. 5223-5231.

Wang, Z., and Eiler, J.M., 2008, Insights into the origin of low-$\delta^{18}O$ basaltic magmas in Hawaii revealed from in situ measurements of oxygen isotope compositions of olivines: Earth and Planetary Science Letters, v. 269, p. 377-387.

Workman, R.K., and Hart, S.R., 2005, Major and trace element composition of the depleted MORB mantle (DMM): Earth and Planetary Science Letters, v. 231, p. 53-72.

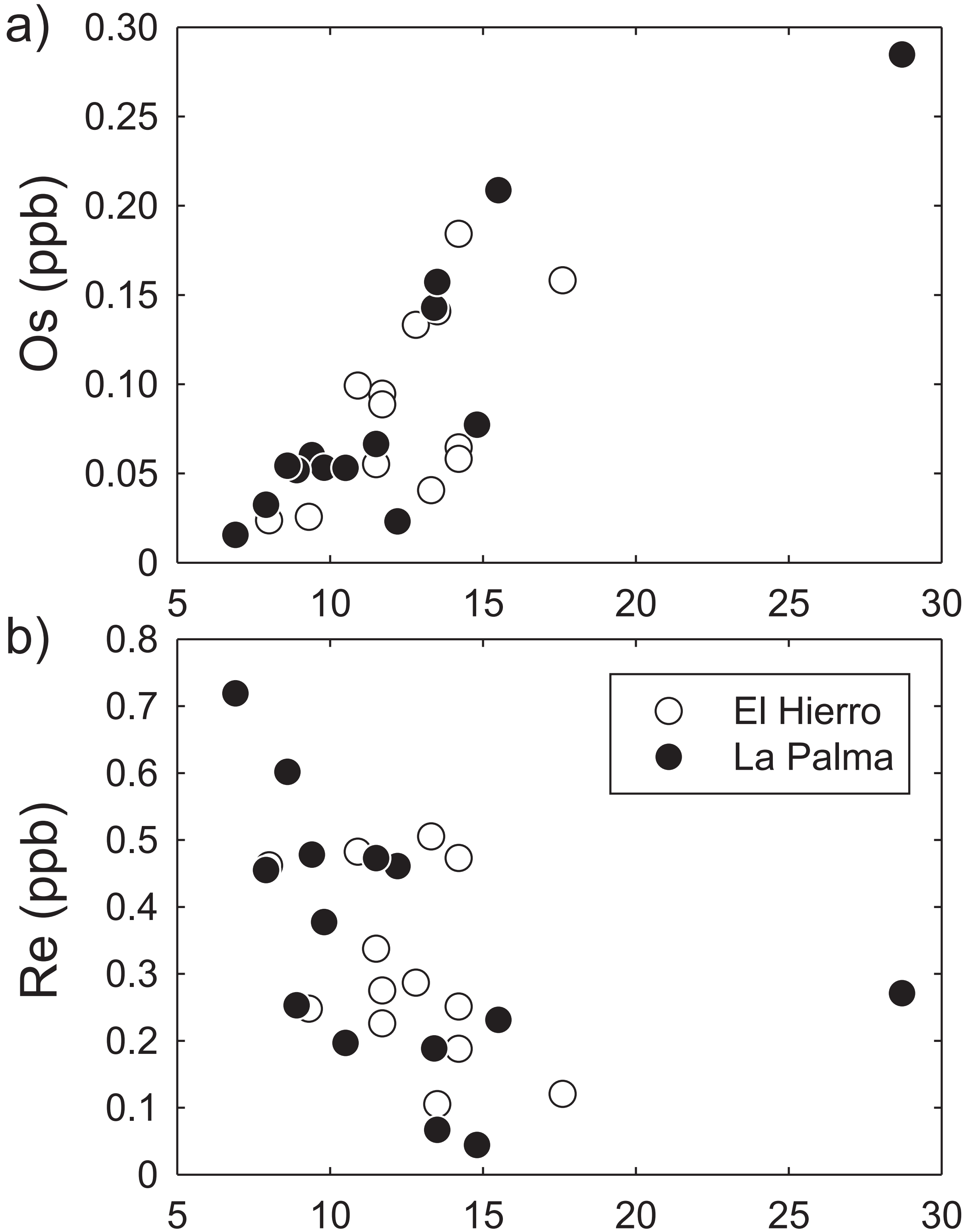

Figure DR1
Day *et al.* (2009)

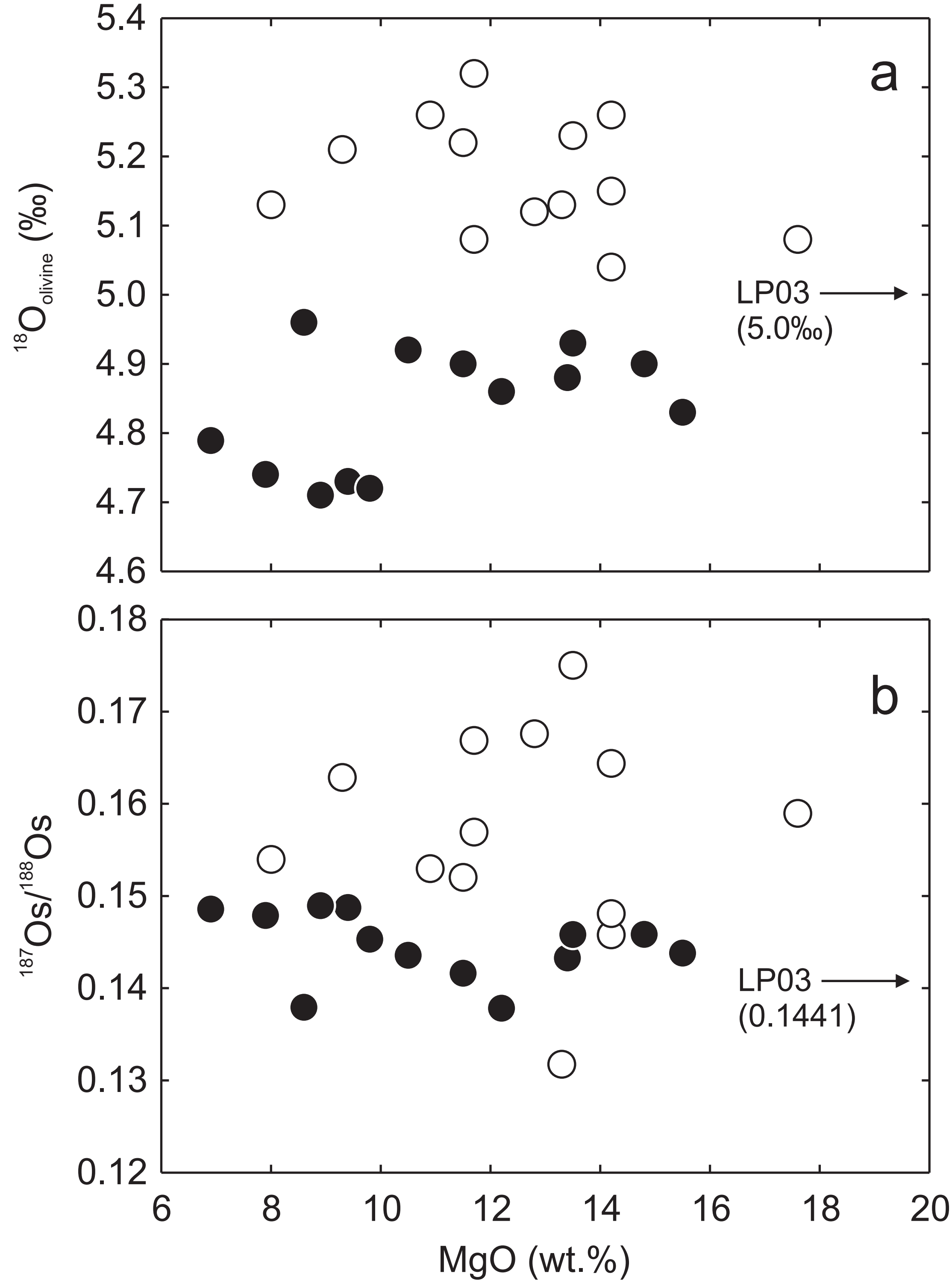

Figure DR2
Day *et al.* (2009)

DATA REPOSITORY ITEM

Table DR1: Locations, olivine compositions and whole-rock major-element compositions of La Palma and El Hierro samples

Sample[a]	UTM Co-ordinates[b]		Olivine[c]	Whole-rock composition (wt.%)[d]											
			Fo (mol.%)	SiO_2	TiO_2	Al_2O_3	$Fe_2O_3^T$	MgO	MnO	CaO	Na_2O	K_2O	P_2O_5	Total	Mg-*no.*
El Hierro, Canary Islands, Spain															
JMDD EH 01	274522	180854	81.3 ±2.6	39.8	5.39	9.21	16.8	14.2	0.21	10.7	1.84	0.77	0.47	98.91	62.6
JMDD EH 03	274736	175528		42.7	3.47	11.5	14.9	12.8	0.21	10.9	2.37	0.76	0.54	99.69	63.1
JMDD EH 07	274608	175517	80.0 ±0.5	43.7	3.30	11.2	13.6	11.7	0.20	11.1	2.14	1.02	0.64	99.21	63.1
JMDD EH 08	274605	175511		43.1	4.65	12.9	14.3	9.27	0.21	10.5	2.79	1.17	0.77	100.1	56.3
JMDD EH 10	274758	175850	78.3 ±0.3	41.4	5.23	9.35	17.8	14.2	0.21	10.0	2.23	0.75	0.67	101.1	61.3
JMDD EH 11	274760	175850	80.5 ±2.3	41.6	5.43	10.5	16.3	11.5	0.22	10.8	2.57	1.01	0.63	100.1	58.3
JMDD EH 12	274802	175849		42.1	3.72	10.7	14.7	13.5	0.20	10.8	2.41	0.68	0.47	99.18	64.6
JMDD EH 13	274805	175848	79.4 ±1.6	40.9	5.15	8.92	17.2	14.2	0.21	10.4	2.33	0.58	0.51	100.1	62.1
JMDD EH 14	274750	175856		42.7	5.61	13.4	15.2	8.03	0.22	10.2	3.61	1.13	0.92	100.3	51.2
JMDD EH 15	274739	175901		42.3	3.02	8.94	15.9	17.6	0.19	9.21	1.72	0.48	0.30	99.29	68.7
JMDD EH 16	274727	175913		43.1	4.03	10.4	14.5	11.7	0.21	12.4	2.42	0.81	0.75	100.5	61.4
JMDD EH 17	273956	175940		41.1	4.34	10.3	15.6	13.3	0.21	11.1	2.68	0.91	0.83	99.54	62.8
JMDD EH 18	274846	175302	79.4 ±2.2	42.0	5.41	11.3	15.3	10.9	0.21	10.1	3.18	0.98	0.64	100.1	58.4
La Palma, Canary Islands, Spain															
JMDD LP 01	284546	174918	81.3 ±1.9	44.0	3.20	10.3	13.6	13.4	0.20	11.4	2.07	0.78	0.39	99.21	66.1
JMDD LP 02	284552	174904		44.6	3.65	12.8	13.3	9.43	0.20	10.6	2.96	1.22	0.62	99.06	58.5
JMDD LP 03	284048	175502	83.3 ±0.8	39.0	1.40	5.40	14.5	28.7	0.22	4.16	<0.01	0.05	0.19	99.84	79.7
JMDD LP 04	284617	175157		43.5	4.87	14.1	13.6	7.90	0.21	10.7	3.35	1.34	0.77	100.1	53.6
JMDD LP 05	284615	175153		41.3	3.97	10.7	15.4	12.2	0.21	11.2	2.40	0.77	0.56	98.71	61.1
JMDD LP 07	284606	175153		42.4	3.84	11.6	14.2	9.79	0.20	12.5	2.75	1.15	0.62	98.83	57.7
JMDD LP 09	284118	175207	84.3 ±1.6	42.0	3.29	11.0	13.8	13.5	0.19	10.9	2.26	0.93	0.50	98.73	66.0
JMDD LP 10	284905	174948		43.8	2.97	9.98	14.1	14.8	0.20	10.5	1.68	0.61	0.33	99.16	67.6
JMDD LP 11	284911	174950	79.3 ±0.7	43.0	3.71	12.7	14.5	8.92	0.20	11.2	2.26	0.94	0.56	98.50	54.9
JMDD LP 14	283526	175428		43.2	3.67	11.7	13.5	11.5	0.19	10.8	3.26	1.30	0.95	99.65	62.7
JMDD LP 15	283531	175438		43.2	3.76	12.5	13.3	10.5	0.19	11.0	3.38	1.59	0.76	99.99	61.0
JMDD LP 19	283656	175041		44.3	4.03	15.1	13.1	6.87	0.21	10.3	4.49	2.08	1.04	100.9	51.0
JMDD LP 24	282825	175138		43.4	3.93	13.3	13.7	8.58	0.20	11.6	3.70	1.70	0.90	100.5	55.4
LPF 96-66	Barranco De Fagundo		82.5 ±3.5	44.6	2.52	9.80	13.0	15.5	0.18	11.3	1.65	0.65	0.32	99.50	70.3

[a]Samples - JMDD series from 2002 field collection. [b]UTM - Garmin GPS. Datum = WGS 84

[c]Average forsterite composition of olivine (Molar Mg/Mg+Fe) based upon 15 to 100 analyses of olivines from each sample (including both core and rim analyses) made using a JEOL JXA-8900 SuperProbe (University of Maryland) operating with a 15kV accelarating voltage and a beam current of 25 nA. Oxide totals for each measurement average 99.5 ±0.8%. Data for LPF 96-66 from Nikogosian *et al.* (2002).

[d]Whole-rock major element data from Day (2004). Measurements by XRF, University of Leicester, UK.

DATA REPOSITORY ITEM

Table DR2: Modeling parameters for O-Os isotopes in Figure 2

Reservoir	Dominant Component*	Age (Ga)	$\delta^{18}O$ (‰)	$^{187}Os/^{188}Os$	[Os] ppb	Model (Fig. 2)	References
DMM		-	5.2	0.124-0.130	3.3	Endmember	[1]
Metasomatised	Pelagic Sediments	-	20.0	2.0	0.5	d	[2]
Mantle Components	Layer-2 Basalt	1.3	5.2	0.83	2.0	b	[3]
	Layer-3 Gabbro (<ROC)	1.3	0.0	0.40	2.0	a	[3]
	Azores Lithosphere	2.5	5.0	0.110	3.3	e	[4]
	Hawai'i Lithosphere	-	0.0	0.124	3.3	c	[2]

* Dominant component within a pyroxenite-enriched peridotite mantle end-member.
[1] Eiler, 2001; Workman & Hart, 2005 [2] Lassiter and Hauri, 1998; [3] Pearson et al., 1991; Eiler, 2001; Pearson and Nowell, 2004; Dale *et al.* 2007; [4] Schaefer *et al.,* 2002; Turner *et al.,* 2007